Relationships between Metal–Metal Force Constants and Metal–Metal Separations for Ag_2 and Pd_2 Systems. Crystal and Molecular Structures of $Ag_2(dmb)_2X_2$ (X = Cl, Br, I; dmb = 1,8-Diisocyano-*p*-menthane) and *cis*-$Pd(CNC(CH_3)_3)_2Cl_2$ Complexes[1]

Daniel Perreault, Marc Drouin, André Michel,*[2a] and Pierre D. Harvey*[2b]

Département de chimie, Université de Sherbrooke, Sherbrooke, Québec, Canada J1K 2R1

Received June 22, 1992

The complexes $Ag_2(dmb)_2X_2$ (X = Cl, Br, I; dmb = diisocyano-*p*-menthane) have been characterized by X-ray diffraction at 233 K (X = Cl), 293 K (X = Br), and 243 K (X = I). The silver complexes are found to contain $Ag_2(dmb)_2^{2+}$ core structures with two silver atoms bridged by dmb ligands to give $Ag_2N_4C_{14}$ rings. The halogen atoms are doubly bridging the silver metals, with Ag–X bond distances of 2.685(3) and 2.719(3) Å (X = Cl), 2.736(3) and 2.836(3) Å (X = Br), and 2.904(1) and 2.935(1) Å (X = I). The Ag–Ag separations are 3.452(2), 3.347(3), and 3.379(2) Å for X = Cl, Br, and I, respectively. The *cis*-$Pd(CNC(CH_3)_3)_2Cl_2$ complex has also been synthesized and characterized by X-ray crystallography; the molecules pack as four quasi-face-to-face dimers, where very weak Pd–Pd interactions are observed (Pd(1)–Pd(1), 4.441(3) Å; Pd(2)–Pd(2), 4.359(3) Å; Pd(3)–Pd(3), 4.056(3) Å; Pd(4)–Pd(4), 4.463(3) Å). The low-frequency (10–400 cm^{-1}) vibrational spectra of these compounds and of four other related complexes containing Ag–Ag and Pd–Pd units in the solid state have been analyzed. Including literature results, for the metal–metal stretching frequencies ($\nu(M_2)$), data banks of nine and twelve points are accumulated for the silver and palladium compounds, respectively, where reparametrized Herschbach–Laurie type relationships (H–L) between $r(M_2)$ and $F(M_2)$, as applied to Ag_2 or Pd_2 systems, are designed. Crystal data: $Ag_2(dmb)_2Cl_2 \cdot 2CHCl_3$, monoclinic, $P2_1/n$, a = 10.8291(11) Å, b = 14.1991(11) Å, c = 12.9318(17) Å, β = 106.437(9)°, V = 1907.2(3) Å^3, Z = 2; $Ag_2(dmb)_2Br_2$, monoclinic, $P2_1/n$, a = 9.6030(7) Å, b = 17.7394(8) Å, c = 17.2335(10) Å, β = 102.932(6)°, V = 2861.3(3) Å^3, Z = 4; $Ag_2(dmb)_2I_2 \cdot CH_3CH_2OH$, monoclinic, $P2_1/n$, a = 9.1781(12) Å, b = 14.9731(15) Å, c = 12.1882(12) Å, β = 96.799(9)°, V = 1663.2(3) Å^3, Z = 2; *cis*-$Pd(CNC(CH_3)_3)_2Cl_2$, triclinic, $P\bar{1}$, a = 12.2675(10) Å, b = 12.334(13) Å, c = 21.211(4) Å, α = 99.663(12)°, β = 99.985(12)°, γ = 90.433(7)°, V = 3113.9(7) Å^3, Z = 8.

Introduction

Empirical equations relating atom–atom distances (r) and atom–atom force constants (F)[3,4] or atom–atom stretching frequencies (ν),[5,6] are numerous. We recently proposed reparametrized Herschbach and Laurie's type relationships ($r = a + b(\log F)$)[3b] that would apply to Ag_2 and Au_2, rather than equations that correlate these parameters for dimeric systems belonging to a specific row of elements in the periodic table.[1] The two major advantages of this new approach are that these equations do not exhibit mathematical limitations due to convergence for small F values (see Woodruff's rules),[4] and are essentially more accurate in many cases since each element is addressed individually.[1] The disadvantage is the rather poor availability of structural and vibrational data for some elements. In our previous work, only four data points were collected to approximate an equation for Ag_2 systems. In order to improve the quality of these new proposed relationships, the number of data needs to be increased, bearing in mind simultaneously that the r range (in which the equations would be applied) should also be as wide as possible. We are currently investigating the photochemical and photophysical properties of the Ag(I), Au(I), and Pd(I) dimers.[7,8] These systems are of interest since they exhibit long-lived lowest energy excited states (0.2–2.4 μs) and their photochemical reactivity and photophysical properties depend, in part, upon M_2 interactions.

The sum of the van der Waals radii is commonly accepted as being the criterion for the presence of M_2 interactions. In the family of weakly interacting dimers, the so-called van der Waals dimers are well-known and are generally found in the vapor phase or in low-temperature matrices.[9] To achieve the synthesis of binuclear systems which specifically exhibit such $r(M_2)$ values, bridging ligands with appropriate bite distances must be employed.[10] In some instances, crystal packings may induce favorable stacking structures involving weak M_2 interactions.[8,11] In these cases $\nu(M_2)$ would appear in the lattice region.

In this work, we wish to report the single-crystal X-ray diffraction structures of three $Ag_2dmb_2X_2$ complexes, (X = Cl, Br, I) and of the *cis*-$Pd(CNC(CH_3)_3)_2Cl_2$ compound in connection with the related *cis*-$Pd(CNR)_2Cl_2$ complexes (R = C_6H_{11},[12] 2,6-$(CH_3)_2$-C_6H_3[13]), that crystallize in a dimeric form (C_{2h} symmetry) with very weak Pd–Pd interactions. Furthermore, we also report

* To whom correspondence should be addressed.

(1) Part 1: Perreault, D.; Drouin, M.; Michel, A.; Miskowski, V. M.; Schaefer, W. P.; Harvey, P. D. *Inorg. Chem.* **1992**, *32*, 695.

(2) (a) All correspondence pertaining to crystallographic studies should be addressed to this author. (b) All other correspondence should be addressed to this author.

(3) (a) Badger, R. M. *J. Chem. Phys.* **1934**, *2*, 128; **1935**, *3*, 710. (b) Hershback, D. R.; Laurie, V. W. *J. Chem. Phys.* **1961**, *35*, 458.

(4) (a) Miskowski, V. M.; Dallinger, R. F.; Christoph, G. G.; Morris, D. E.; Spies, G. H.; Woodruff, W. H. *Inorg. Chem.* **1987**, *26*, 2127. (b) Conradson, S. D.; Sattelberger, A. P.; Woodruff, W. H. *J. Am. Chem. Soc.* **1988**, *110*, 1309. (c) Woodruff, W. H. Unpublished results.

(5) (a) Butler, I. S.; Harvey, P. D.; McCall, J. M.; Shaver, A. *J. Raman Spectrosc.* **1986**, *17*, 221. (b) Stendal, R. *Z. Naturforsch.* **1975**, *30B*, 281.

(6) Cordier, C. Ph.D. Thesis, Université Paris VI, 1991.

(7) Perreault, D.; Drouin, M.; Michel, A.; Harvey, P. D. *Inorg. Chem.* **1991**, *30*, 2.

(8) Perreault, D.; Drouin, M.; Michel, A.; Harvey, P. D. *Inorg. Chem.* **1992**, *31*, 2740.

(9) (a) Huber, K. P.; Herzberg, G. *Molecular Spectra and Molecular Structure Constants of Diatomic Molecules*; Van Nostrand: New York, 1979. (b) Miller, J. C.; Andrews, L. *Appl. Spectrosc. Rev.* **1980**, *16*, 1. (c) See also for examples: Borysow, A.; Grycuk, T. *Physica* **1982**, *114C*, 414.

(10) Che, C.-M.; Wong, W. T.; Lai, T.-F.; Kwong, H.-L. *J. Chem. Soc., Chem. Commun.* **1989**, 243.

(11) The $[Rh(CNC_6H_5)_4]^+$ complex oligomerizes in solutions with increased concentration. The solid-state structure also consists of quasi-linear stacking: Miller, J. S., Ed. *Extended Linear Chain Compounds*; Plenum: New York, 1983; Vol. 1.

0020-1669/93/1332-1903$04.00/0

Table I. Crystallographic Data for $Ag_2(dmb)_2X_2$ (X = Cl, Br, I) and *cis*-$Pd(CNC(CH_3)_3)_2Cl_2$

chem formula	$Ag_2Cl_2C_{24}H_{36}N_4 \cdot 2CHCl_3$	$Ag_2Br_2C_{24}H_{36}N_4$	$Ag_2I_2C_{24}H_{36}N_4 \cdot CH_3CH_2OH$	$PdCl_2C_{10}H_{18}N_2$
fw	905.99	756.13	896.20	343.57
space group	$P2_1/n$	$P2_1/n$	$P2_1/n$	$P\bar{1}$
T, K	233	293	243	293
a, Å	10.8291(11)	9.6030(7)	9.1781(12)	12.2675(10)
b, Å	14.1991(11)	17.7394(8)	14.9731(15)	12.334(13)
c, Å	12.9318(17)	17.2335(10)	12.1882(12)	21.211(4)
α, deg				99.663(13)
β, deg	106.437(9)	102.932(6)	96.799(9)	99.985(12)
γ, deg				90.433(7)
V, Å^3	1907.2(3)	2861.3(3)	1663.2(3)	3113.9(7)
Z	2	4	2	8
λ, Å	0.706 90	0.706 90	0.706 90	0.706 90
ρ_{calcd}, g cm^{-3}	1.578	1.755	1.790	1.466
μ, cm^{-1}	16.05	41.41	30.27	15.00
R^a	0.059	0.065	0.043	0.080
$R_w{}^b$	0.046	0.053	0.052	0.067

^{a} $R = \sum(F_o - F_c)/\sum F_o$. ^{b} $R_w = [\sum w(F_o - F_c)^2/\sum(wF_o^2)]^{1/2}$. $w = (\sigma^2(F) + 0.0002F^2)^{-1}$.

the low-frequency (10–400 cm^{-1}) solid-state Raman spectra for these compounds along with two other related Ag_2 complexes for which the $r(Ag_2)$ values are known. Using literature data for other M_2 compounds, reparametrized Herschbach–Laurie type relationships (H–L) applied to silver and palladium polynuclear complexes will now be presented.

Experimental Section

Materials. $Ag_2(C_6H_5NNNC_6H_5)_2$,[14] *cis*-$Pd(CN\text{-}2,6\text{-}(CH_3)_2C_6H_3)_2Cl_2$,[13] *cis*-$Pd(CNC_6H_{11})_2Cl_2$,[12] and dmb[15] were prepared according to standard procedures. $Ag_2(O_2CCF_3)_2$ was purchased from Strem Chemical Co. and was slowly recrystallized in acetonitrile and kept in the dark when not in use.[16] AgCl, AgBr, and AgI were prepared from the direct reaction of $AgNO_3$ with the appropriate NaX salt (X = Cl, Br, I) in water and dried in vacuo for several days. The purity was checked by elemental analysis.

$Ag_2(dmb)_2Cl_2$. AgCl (0.287 g, 2 mmol) was suspended in a benzene solution containing an excess of dmb (0.761 g, 4 mmol), and stirred at 40 °C for several hours. After the solution was cooled to room temperature, the white solid was filtered off, washed with ether, and recrystallized three times from acetonitrile/ether solution (yield 70–80%). [Anal. Calcd for $Ag_2C_{24}H_{36}N_4Cl_2$: C, 43.2; H, 5.44; N, 8.44; Ag, 32.3; Cl, 10.6. Found: C, 43.1; H, 5.36; N, 8.22; Ag, 31.9; Cl, 10.4.] NMR (CD_3CN; 298 K): δ (ppm) = 1.48 s (6H) and 1.46 s (3H) for CH_3, 1.51 m, 1.52 m, 1.55 m, and 1.59 m (9H) for CH_2 and CH groups. IR (NaCl disk): 2179 cm^{-1} (ν(N≡C)). Raman (solid powder): 2177 cm^{-1} (ν(N≡C)). Crystals suitable for X-ray crystallography were obtained from slow diffusion of chloroform into a concentrated solution of acetonitrile kept at 268 K (refrigerator at −5 °C) followed by a slow evaporation of the solutions at the same temperature.

$Ag_2(dmb)_2Br_2$. The complex was prepared in the same way as for $Ag_2(dmb)_2Cl_2$, except that AgBr was used instead of AgCl (yield 70–80%). [Anal. Calcd for $Ag_2C_{24}H_{36}N_4Br_2$: C, 38.1; H, 4.80; N, 7.41; Ag, 28.5; Br, 21.1. Found: C, 37.4; H, 4.46; N, 7.89; Ag, 29.1; Br, 21.0.] NMR (CD_3CN; 298 K): δ(ppm) = 1.47 s (6H) and 1.46 s (3H) for CH_3; 1.52 m and 1.56 m (9H) for CH_2 and CH. IR (KBr disk): 2176 cm^{-1} (ν(N≡C)). Raman (solid powder): 2181 cm^{-1} (ν(N≡C)). Crystals suitable for X-ray crystallography were obtained by slow evaporation of a concentrated solution in acetonitrile at 298 K.

$Ag_2(dmb)_2I_2$. The complex was prepared in the same way as for $Ag_2(dmb)_2Cl_2$, except that AgI was used instead of AgCl (yield 70–80%). [Anal. Calcd for $Ag_2C_{24}H_{36}N_4I_2$: C, 33.9; H, 4.27; N, 6.59; Ag, 25.4; I, 29.9. Found: C, 33.2; H, 4.28; N, 6.13; Ag, 25.0; I, 29.5.] NMR (CD_3CN; 298 K): δ (ppm) = 1.49 s (6H) and 1.48 s (3H) for CH_3, 1.56 m, br (9H) for CH_2 and CH. IR (CsI disk): 2176 cm^{-1} (ν(N≡C)). Crystals suitable for X-ray crystallography were obtained by slowly cooling a saturated solution in ethanol, prepared at 298 K, down to 268 K. The process took several days.

***cis*-$Pd(CNC(CH_3)_3)_2Cl_2$.** The complex was prepared and purified according to the literature procedure outlined for *cis*-$Pd(CNC_6H_{11})_2Cl_2$, except that $CNC(CH_3)_3$ (Aldrich Chem. Co.) was used instead of CNC_6H_{11}. The white solid was slowly crystallized from a concentrated solution in acetonitrile and identified by X-ray crystallography. The crystals used for the micro-Raman studies were the same as for the X-ray ones.

Instruments. The Raman spectra were measured on two different spectrometers. The first one was used for all the solid samples and was an Instruments SA Raman spectrometer equipped with a U-1000 Jobin-Yvon 1.0-m double monochromator using either the 647.1-nm red line or the 514.5-nm green line of Spectra-Physics krypton and argon ion lasers, respectively, for excitation. The second one was used for the $Ag_2(dmb)_2X_2$ (X = Br, I) samples, and was an IFS 66/CS FT-IR spectrometer coupled with an FRA 106 FT-Raman module using a Nd:YAG laser (1064) nm excitation) and a notch filter (cutoff ~ 70 cm^{-1}). The far-IR spectra were measured on an FT-BOMEM DA 3.002 spectrometer with a resolution of 4 cm^{-1}, typically using from 50 to 256 scans.

Crystallographic Data. For all four structures, data were collected on an Enraf-Nonius CAD-4 diffractometer using graphite-monochromated, Mo Kα radiation (λ = 0.710 73 Å), and the $\omega/2\theta$ scan method was used. The NRCVAX[17] system was used for all calculations. For all four compounds, direct methods followed by Fourrier synthesis were used to locate all non-hydrogen atoms. The crystallographic data and the final coordinates and β values for non-H atoms with esd's are presented in Tables I and II, respectively.

$Ag_2(dmb)_2Cl_2 \cdot 2CHCl_3$. A colorless prismatic crystal was mounted at low temperature under an argon atmosphere, and the data were collected at 233 K at a constant speed of 2.7° min^{-1}; two standards were monitored every 30 min, showing a 20% decay which was later corrected for in data reduction. Crystal data: M = 786.61, monoclinic, $P2_1/n$, a = 10.8291(11) Å, b = 14.1991(11) Å, c = 12.9318(17) Å, β = 106.437(9)°, V = 1907.2(3) Å^3, Z = 2, D_{calc} = 1.578 g cm^{-3}, μ = 16.05 cm^{-1}. The lattice parameters were refined from 24 reflections in the range 30° ≤ 2θ ≤ 40°. A total of 2483 unique reflections were measured, of which 1448 were considered to be observed with $I_{net} \geq 2.50\sigma I_{net}$. The molecules crystallize on centers of symmetry and the DMB groups are disordered; the population parameter was refined to 0.68(1) for one orientation and to (1 − 0.68) for the other. The disorder results in the near superimposition of C(2), C(4), C(6), and C(8), which were represented as single atoms; their population were set to 1 and set with anisotropic temperature factors. The Ag, Cl, N, C(1), and C(9) atoms and the chloroform molecule were

(12) Kinato, Y.; Hori, T. *Acta Crystallogr.* **1981**, *B37*, 1919.
(13) Drouin, M.; Perreault, D.; Harvey, P. D.; Michel, A. *Acta Crystallogr. C* **1991**, *C47*, 752.
(14) Beck, J.; Strahle, J. *Z. Naturforsch. B: Anorg. Chem., Org. Chem.* **1986**, *41B*, 4.
(15) Weber, W. P.; Gokel, G. W.; Ugi, I. K. *Angew. Chem., Int. Ed. Engl.* **1972**, *11*, 530.
(16) Griffin, R. G.; Ellett, J. D., Jr.; Mehring, M.; Bullitt, J. G.; Waugh, J. S. *J. Chem. Phys.* **1972**, *57*, 2147.
(17) (a) Larson, A. C. *Acta Crystallogr.* **1967**, *23*, 664. (b) Gabe, E. J.; LePage, Y.; Charland, J.-P.; Lee, F. L. NRCVAX. An Interactive Program System for Structure Analysis. *J. Appl. Crystallogr.* **1989**, *22*, 384. (c) Cromer, D. T.; Waber, J. T. In *International Tables for X-Ray Crystallography*; Ibers, J. A., Hamilton, W. C., Eds.; Kynoch Press: Birmingham, England, 1974; Vol. IV, Table 2.2B, pp 99–101 (present distributor: Kluwer Academic Publishers, Dordrecht, The Netherlands). (d) LePage, Y. *J. Appl. Crystallogr.* **1988**, *21*, 983. (e) Johnson, C. K. *ORTEP. A Fortran Thermal Ellipsoid Plot Program*; Technical Report ORNL-5138; Oak Ridge National Laboratory: Oak Ridge, TN, 1976.

Table II. Final Coordinates and B Values for Non-H Atoms with Esd's in Parentheses

atom	x	y	z	B_{eq},[a] Å^2	atom	x	y	z	B_{eq},[a] Å^2
				$Ag_2(dmb)_2Cl_2{\cdot}CHCl_3$					
Ag	0.01702(9)	0.05488(6)	0.88571(7)	4.91(4)	C(4)	0.0656(10)	0.2913(7)	1.1928(8)	5.0(6)
Cl(1)	0.1833(3)	−0.05679(24)	1.02636(22)	5.72(16)	C(5)	0.2024(14)	0.3024(10)	1.1854(11)	4.1(3)
Cl(2)	0.4861(4)	0.0336(3)	0.1334(3)	9.8(3)	C(6)	0.2857(9)	0.2167(7)	1.2289(9)	4.9(6)
Cl(3)	0.6893(4)	0.1635(3)	0.2236(3)	11.3(3)	C(7)	−0.2872(15)	−0.1954(11)	0.6510(12)	4.6(4)
Cl(4)	0.7280(4)	−0.0353(3)	0.2592(4)	11.3(3)	C(8)	0.2036(10)	0.3287(7)	1.0680(8)	5.1(6)
N(1)	−0.0969(8)	−0.1017(6)	0.7004(7)	5.1(5)	C(9)	0.1001(10)	0.1891(7)	0.9429(8)	5.1(6)
N(2)	0.1432(8)	0.2509(6)	0.9937(6)	5.0(5)	C(10)	0.3399(16)	0.3369(12)	1.0547(13)	6.0(4)
C(1)	−0.0559(10)	−0.0406(7)	0.7559(8)	5.2(6)	C(11)	0.1291(16)	0.4150(12)	1.0292(13)	6.3(5)
C(2)	−0.1532(10)	−0.1884(8)	0.6396(8)	5.1(6)	C(12)	−0.1602(16)	−0.1697(12)	0.5231(13)	6.2(4)
C(3)	−0.0701(15)	−0.2664(11)	0.6897(13)	5.3(4)	C(13)	0.6507(12)	0.0512(11)	0.1666(10)	8.1(8)
				$Ag_2(dmb)_2Br_2$					
Ag(1)	0.6964(21)	0.73494(11)	0.25440(12)	4.59(11)	C(9)	−0.2273(24)	0.7485(13)	0.0159(12)	4.9(15)
Ag(2)	−0.02946(21)	0.79834(11)	0.06724(12)	4.61(11)	C(10)	−0.5099(25)	0.6316(13)	−0.0609(13)	5.2(15)
Br(1)	0.1265(3)	0.66921(15)	0.12126(17)	5.17(16)	C(11)	−0.592(3)	0.7496(14)	−0.0101(16)	6.3(17)
Br(2)	−0.1209(3)	0.85584(14)	0.20083(16)	4.66(15)	C(12)	−0.358(3)	0.5640(14)	0.3367(15)	5.8(17)
N(1)	−0.2105(17)	0.6387(9)	0.2728(10)	3.6(11)	C(13)	0.1251(23)	0.8874(12)	0.0598(13)	3.8(14)
N(2)	−0.3411(17)	0.7222(9)	0.0094(9)	3.1(10)	C(14)	0.3085(24)	0.9923(12)	0.1001(14)	4.0(14)
N(3)	0.2055(18)	0.9335(10)	0.0761(10)	3.5(11)	C(15)	0.453(3)	0.9588(14)	0.1323(14)	4.9(15)
N(4)	0.3336(18)	0.8428(9)	0.3319(10)	3.6(10)	C(16)	0.4641(22)	0.9118(12)	0.2066(14)	3.9(14)
C(1)	−0.1036(21)	0.6653(11)	0.2766(12)	3.0(12)	C(17)	0.4115(22)	0.9562(12)	0.2730(12)	3.2(12)
C(2)	−0.3530(22)	0.6067(12)	0.2595(12)	3.0(12)	C(18)	0.2693(24)	0.9898(11)	0.2395(13)	3.0(13)
C(3)	−0.4573(24)	0.6675(14)	0.2346(15)	5.5(17)	C(19)	0.2610(23)	1.0372(12)	0.1617(13)	4.1(14)
C(4)	−0.4598(22)	0.7073(12)	0.1568(12)	3.5(13)	C(20)	0.4275(22)	0.9075(13)	0.3496(12)	3.7(13)
C(5)	−0.4772(22)	0.6492(13)	0.0884(13)	4.1(15)	C(21)	0.2547(23)	0.7955(13)	0.3122(11)	3.6(13)
C(6)	−0.3723(24)	0.5888(12)	0.1096(13)	3.8(14)	C(22)	0.571(3)	0.8860(14)	0.3869(15)	6.6(17)
C(7)	−0.369(3)	0.5507(13)	0.1890(13)	4.8(15)	C(23)	0.368(3)	0.9528(13)	0.4143(14)	5.0(15)
C(8)	−0.4810(22)	0.6855(12)	0.0080(13)	3.5(13)	C(24)	0.307(3)	1.0408(13)	0.0295(13)	5.4(16)
				$Ag_2(dmb)_2I_2{\cdot}CH_3CH_2OH$					
Ag	0.84450(9)	0.43884(4)	0.97892(6)	3.97(3)	C(7)	0.6289(14)	0.6763(8)	0.6937(10)	3.7(3)
I	1.06631(9)	0.44820(5)	0.82798(5)	4.68(3)	C(8)	1.0305(11)	0.1856(6)	1.1738(8)	4.3(5)
N(2)	0.9518(9)	0.2539(5)	1.1046(6)	3.8(4)	C(9)	0.8957(11)	0.3097(6)	1.0541(8)	3.9(5)
N(1)	0.6183(9)	0.5810(5)	0.8527(6)	3.5(3)	C(10)	1.0243(16)	0.0982(10)	1.1103(11)	5.3(3)
C(1)	0.6763(10)	0.5238(6)	0.8964(8)	3.4(4)	C(11)	0.9580(16)	0.1765(9)	1.2768(12)	5.2(3)
C(2)	0.5501(11)	0.6609(6)	0.7962(8)	3.8(5)	C(12)	0.3885(16)	0.6384(9)	0.7581(12)	5.4(3)
C(3)	0.5726(14)	0.7373(8)	0.8747(10)	3.9(3)	C(13)	0.469(4)	0.032(3)	0.979(5)	17.0(9)
C(4)	1.2653(12)	0.2347(6)	1.0951(8)	4.2(5)	C(14)	0.386(5)	−0.055(4)	0.997(5)	17.0(9)
C(5)	1.1942(13)	0.2174(8)	1.1986(9)	3.3(2)	O	0.624(4)	0.0112(24)	0.971(3)	17.0(9)
C(6)	1.2073(11)	0.2991(6)	1.2755(7)	3.6(4)					
				cis-$Pd(CNC(CH_3)_3)_2Cl_2$					
Pd(1)	0.97150(13)	0.82995(13)	0.94431(8)	3.93(8)	C(11)	0.5699(15)	0.3463(17)	0.0529(9)	4.9(11)
Pd(2)	0.49968(13)	0.32436(13)	−0.03775(7)	3.73(8)	C(12)	0.6778(15)	0.3853(17)	0.1718(8)	4.7(12)
Pd(3)	0.83589(13)	0.47964(13)	0.46279(7)	3.75(8)	C(13)	0.5911(18)	0.4323(18)	0.2120(9)	6.0(13)
Pd(4)	0.32615(13)	−0.00075(13)	0.44690(8)	4.04(8)	C(14)	0.7658(17)	0.4677(19)	0.1750(10)	6.6(15)
Cl(1)	0.9814(5)	0.7848(5)	0.8357(3)	6.7(4)	C(15)	0.7263(23)	0.2757(21)	0.1900(11)	8.7(18)
Cl(2)	1.1309(5)	0.7417(5)	0.9740(3)	6.2(3)	C(16)	0.6181(16)	0.3990(14)	−0.0590(9)	4.1(10)
Cl(3)	0.3597(4)	0.2303(5)	−0.0092(3)	5.6(3)	C(17)	0.7918(18)	0.5019(17)	−0.0860(11)	6.0(13)
Cl(4)	0.4237(5)	0.2913(5)	−0.14621(25)	5.7(4)	C(18)	0.8623(17)	0.5592(18)	−0.0193(10)	6.4(13)
Cl(5)	0.8123(5)	0.4995(5)	0.3561(3)	6.5(4)	C(19)	0.8590(20)	0.4091(20)	−0.1180(11)	7.5(7)
Cl(6)	0.7426(5)	0.6359(4)	0.4910(3)	5.6(3)	C(20)	0.7445(17)	0.5818(17)	−0.1335(10)	5.4(12)
Cl(7)	0.2369(5)	−0.1427(5)	0.4763(3)	6.1(4)	C(21)	0.3542(16)	0.0688(16)	0.5386(11)	5.7(13)
Cl(8)	0.2818(5)	−0.0701(5)	0.3375(3)	6.1(3)	C(22)	0.3741(17)	0.1709(16)	0.6574(8)	4.7(12)
N(1)	0.9373(12)	0.8699(12)	1.0846(7)	4.2(9)	C(23)	0.4131(23)	0.0860(21)	0.7013(10)	9.2(17)
N(2)	0.7597(13)	0.9492(13)	0.9077(7)	4.7(9)	C(24)	0.2675(19)	0.2174(16)	0.6671(10)	6.2(13)
N(3)	0.6170(12)	0.3644(12)	0.1044(7)	4.3(9)	C(25)	0.4539(18)	0.2640(18)	0.6678(11)	6.4(15)
N(4)	0.6900(12)	0.4447(12)	−0.0715(7)	4.3(8)	C(26)	0.3998(18)	0.1246(17)	0.4270(10)	5.6(13)
N(5)	0.3642(12)	0.1170(13)	0.5912(8)	4.8(9)	C(27)	0.5055(19)	0.2894(17)	0.3980(10)	6.4(13)
N(6)	0.4465(14)	0.1954(13)	0.4159(7)	5.1(10)	C(28)	0.5482(20)	0.3607(18)	0.4608(14)	8.8(19)
N(7)	0.8674(12)	0.4358(13)	0.6034(7)	4.5(9)	C(29)	0.5961(18)	0.2419(18)	0.3625(10)	6.0(14)
N(8)	0.9473(13)	0.2642(12)	0.4198(7)	4.5(9)	C(30)	0.4233(24)	0.3578(23)	0.3665(14)	10.5(9)
C(1)	0.9557(18)	0.8620(16)	1.0323(9)	5.3(13)	C(31)	0.8552(16)	0.4566(16)	0.5539(9)	4.6(12)
C(2)	0.9157(15)	0.8750(15)	1.1552(8)	3.8(10)	C(32)	0.8639(17)	0.4195(16)	0.6704(8)	4.6(12)
C(3)	1.0274(18)	0.9113(18)	1.1994(9)	5.7(13)	C(33)	0.7511(18)	0.3806(18)	0.6739(9)	6.0(13)
C(4)	0.8218(19)	0.9548(19)	1.1596(12)	7.5(16)	C(34)	0.9102(17)	0.5293(15)	0.7126(10)	5.0(12)
C(5)	0.8778(17)	0.7679(19)	1.1600(9)	5.9(13)	C(35)	0.9502(20)	0.3280(19)	0.6787(10)	7.0(15)
C(6)	0.8394(15)	0.9054(16)	0.9194(8)	4.1(10)	C(36)	0.9093(16)	0.3443(16)	0.4406(9)	4.9(12)
C(7)	0.6544(17)	1.0056(18)	0.8872(11)	6.2(14)	C(37)	0.9960(17)	0.1656(16)	0.4040(10)	5.4(12)
C(8)	0.6162(21)	1.0501(24)	0.9517(14)	10.8(20)	C(38)	1.0506(20)	0.1196(18)	0.4576(12)	7.7(15)
C(9)	0.575(3)	0.916(3)	0.8461(16)	13.1(11)	C(39)	1.0761(20)	0.1786(19)	0.3593(12)	7.8(17)
C(10)	0.6850(18)	1.0967(20)	0.8579(11)	7.2(15)	C(40)	0.9068(25)	0.0865(25)	0.3650(15)	12.0(10)

[a] $B_{eq} = (8\pi^2/3)\sum_i\sum_j U_{ij}a_i^*a_j^*a_ia_j$.

also set with anisotropic temperature factors for refinement; other atoms were set with isotropic temperature factors. Distances and angles involving the disordered dmb groups show large deviation from expected values; clearly our model does not represent the situation well. The final residual densities were located near the Ag atoms. The hydrogens were all calculated and not refined (C–H = 1.08 Å).

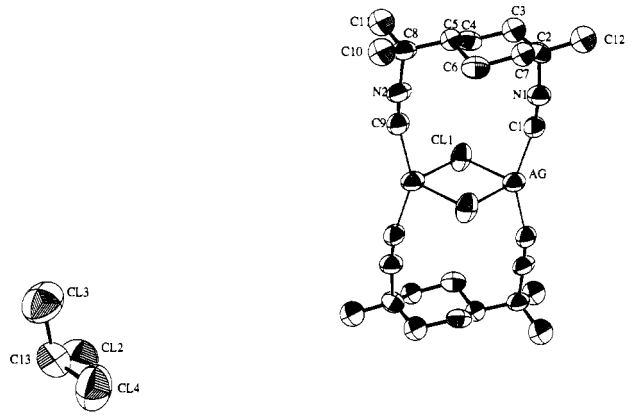

Figure 1. Molecular structure and atom labeling for $Ag_2(dmb)_2Cl_2 \cdot 2CHCl_3$. The ORTEP[17e] drawing is shown with 50% probability ellipsoids.

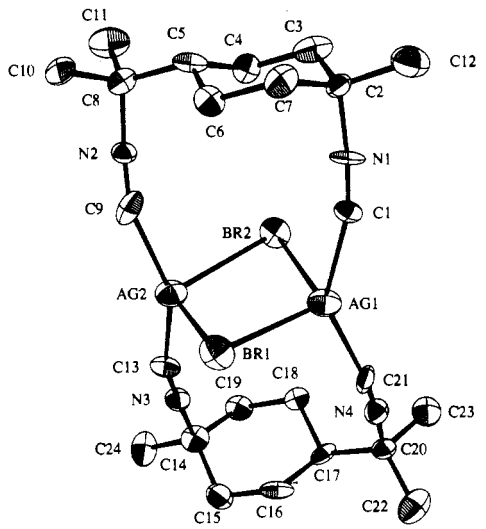

Figure 2. Molecular structure and atom labeling for $Ag_2(dmb)_2Br_2$. The ORTEP[17c] drawing is shown with 50% probability ellipsoids.

$Ag_2(dmb)_2Br_2$. A colorless needle-shaped crystal was mounted at 298 K, and the data were collected at this same temperature at a constant speed of 2.7° min^{-1}. Two standards were monitored every 60 min and showed no significant decay. Crystal data: M = 756.13, monoclinic $P2_1/n$, a = 9.6030(7) Å, b = 17.7394(8) Å, c = 17.2335(10) Å, β = 102.932(6)°, V = 2861.3(3) Å^3, Z = 4, D_{calc} = 1.755 g cm^{-3}, μ = 41.41 cm^{-1}. The lattice parameters were refined from 24 reflections in the range $30 \le 2\theta \le 40°$. A total of 3688 unique reflections were measured, of which 1573 were considered to be observed with $I_{net} \ge 2.5\sigma I_{net}$. The hydrogens were all calculated but not refined (C–H = 1.08 Å). Absorption corrections were applied using interpolation methods from the ABSORP program of NRCVAX.

$Ag_2(dmb)_2I_2 \cdot CH_3CH_2OH$. A colorless prismatic crystal, with tendency to lose solvent, was mounted in a capillary tube with its mother liquor at low temperature under an argon atmosphere for data collection at 243 K. Crystal data: M = 896.20, monoclinic $P2_1/n$, a = 9.1781(12) Å, b = 14.9731(15) Å, c = 12.1882(12) Å, β = 96.799(9)°, V = 1663.2(3), Z = 2, D_{calc} = 1.790 g cm^{-3}, μ = 30.27 cm^{-1}. The lattice parameters were refined from 24 reflections in the range $25 \le 2\theta \le 35°$. A total of 2153 unique reflections were measured, of which 1677 were considered to be observed with $I_{net} \ge 2.5\sigma I_{net}$. Absorption corrections were applied using interpolation methods from the ABSORP program of NRCVAX. As in $Ag_2(dmb)_2Cl_2$, the molecule crystallizes on centers of symmetry and the dmb groups are disordered; the same approach was used for treating the disorder. The occupancy refinement of the orientation population gives 0.778(6) and 1 – 0.778. The hydrogens were all calculated and not refined (C–H = 1.08 Å). The ethanol molecule is located very close to a center of symmetry. The molecule was found to be disordered; the CH_3 and OH parts almost superimpose themselves by symmetry operator. We first used dual scattering factors of half-oxygen and half-carbon at this position, but geometry and huge isotropic thermal parameters found after refinement suggest that our model was not correct. We then decided to use a rigid geometry and isotropic group factors for refinement.

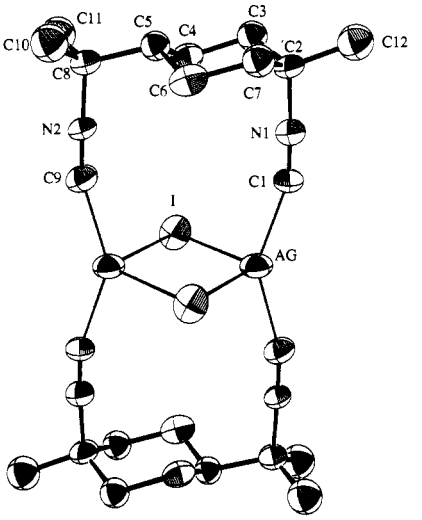

Figure 3. Molecular structure and atom labeling for $Ag_2(dmb)_2I_2$. The ORTEP[17e] drawing is shown with 50% probability ellipsoids.

Table III. Selected Bond Lengths (Å) for $Ag_2(dmb)_2X_2$ Complexes (X = Cl, Br, I)

$Ag_2(dmb)_2Cl_2$		$Ag_2(dmb)_2Br_2$		$Ag_2(dmb)_2I_2$	
Ag–Ag	3.451(2)	Ag–Ag	3.345(1)	Ag–Ag	3.378(2)
Ag–Cl(1)	2.685(4)	Ag(1)–Br(1)	2.736(3)	Ag–I	2.9040(1)
Ag–Cl(1)$_a$	2.719(3)	Ag(1)–Br(2)	2.836(3)	Ag–I(a)	2.935(1)
Ag–C(1)	2.128(10)	Ag(2)–Br(1)	2.781(3)	Ag–C(1)	2.156(9)
Ag–C(9)	2.148(10)	Ag(2)–Br(2)	2.831(3)	Ag–C(9)	2.167(9)
N(1)–C(1)	1.14(13)	Ag(1)–C(1)	2.17(2)	N(1)–C(1)	1.110(11)
N(2)–C(9)	1.16(13)	Ag(1)–C(21)	2.12(2)	N(2)–C(9)	1.126(11)
		Ag(2)–C(9)	2.10(2)		
		Ag(2)–C(13)	2.19(2)		
		N(1)–C(1)	1.12(3)		
		N(2)–C(9)	1.17(3)		
		N(3)–C(13)	1.12(3)		
		N(4)–C(21)	1.13(3)		

***cis*-$PdCl_2(CNC(CH_3)_3)_2$.** A colorless prismatic crystal was obtained by slow evaporation from acetonitrile. Data were collected at 293 K at a constant speed of 4° min^{-1}; four standards monitored every 60 min showed no significant decay. Crystal data: M = 343.57, triclinic $P\bar{1}$, a = 12.2675(10) Å, b = 12.3346(13) Å, c = 21.211(4) Å, α = 99.663(12)°, β = 99.985(12)°, γ = 90.433(7)°, V = 3113.9(7) Å^3, Z = 8, D_{calc} = 1.466 g cm^{-3}, μ = 15.00 cm^{-1}. The lattice parameters were refined from 20 reflections in the range $25 \le 2\theta \le 30°$. A total of 7974 unique reflections were measured of which 5065 were considered to be observed with $I_{net} \ge 2.5\sigma I_{net}$. The space group $P\bar{1}$ was confirmed by the application of MISSYM.[17] The hydrogen atoms were all calculated and not refine (C–H = 1.08 Å).

Results

Structure Descriptions. The $Ag_2(dmb)_2X_2$ complexes (X = Cl, Br, I) exhibit a $Ag_2(dmb)_2^{2+}$ core structure with two silver atoms bridged by the dmb ligands (trans to each other) to give $Ag_2C_{14}N_4$ rings (counting only one side of the cyclohexyl groups). The compounds exhibit further Ag–Ag bridgings with two halogen atoms bridging on each face of the complexes (Figures 1–3). The $Ag_2(dmb)_2^{2+}$ moities are planar for the chloro and iodo derivatives (C_{2h} point group), but a "butterfly" geometry is observed for the bromo analogue (C_1 point group); the angle between the two Ag_2C_2 planes is 10.5(6)°.[18] The intramolecular $r(Ag_2)$ values

(18) The equation for the Ag(1)–Ag(2)–C(13)–C(21), Ag(1)–Ag(2)–C(1)–C(9), and Ag(1)–Br(1)–Ag(2)–Br(2) planes are $-6.44(5)x + 12.08(9)y + 7.508(14)z = 10.34(7)$, $-5.04(6)x + 13.99(7)y + 7.398(16)z = 11.82(5)$, and $7.640(5)x + 10.399(13)y - 0.503(15)z = 7.986(10)$, with χ^2 of 1.773, 14.082, and 2800.924, respectively. While the Ag_2Br_2 unit is not perfectly planar, the Ag_2C_2 units are reasonably planar, where the deviation distances from the planes for the C atoms range from +0.02(3) to –0.08(3) Å.

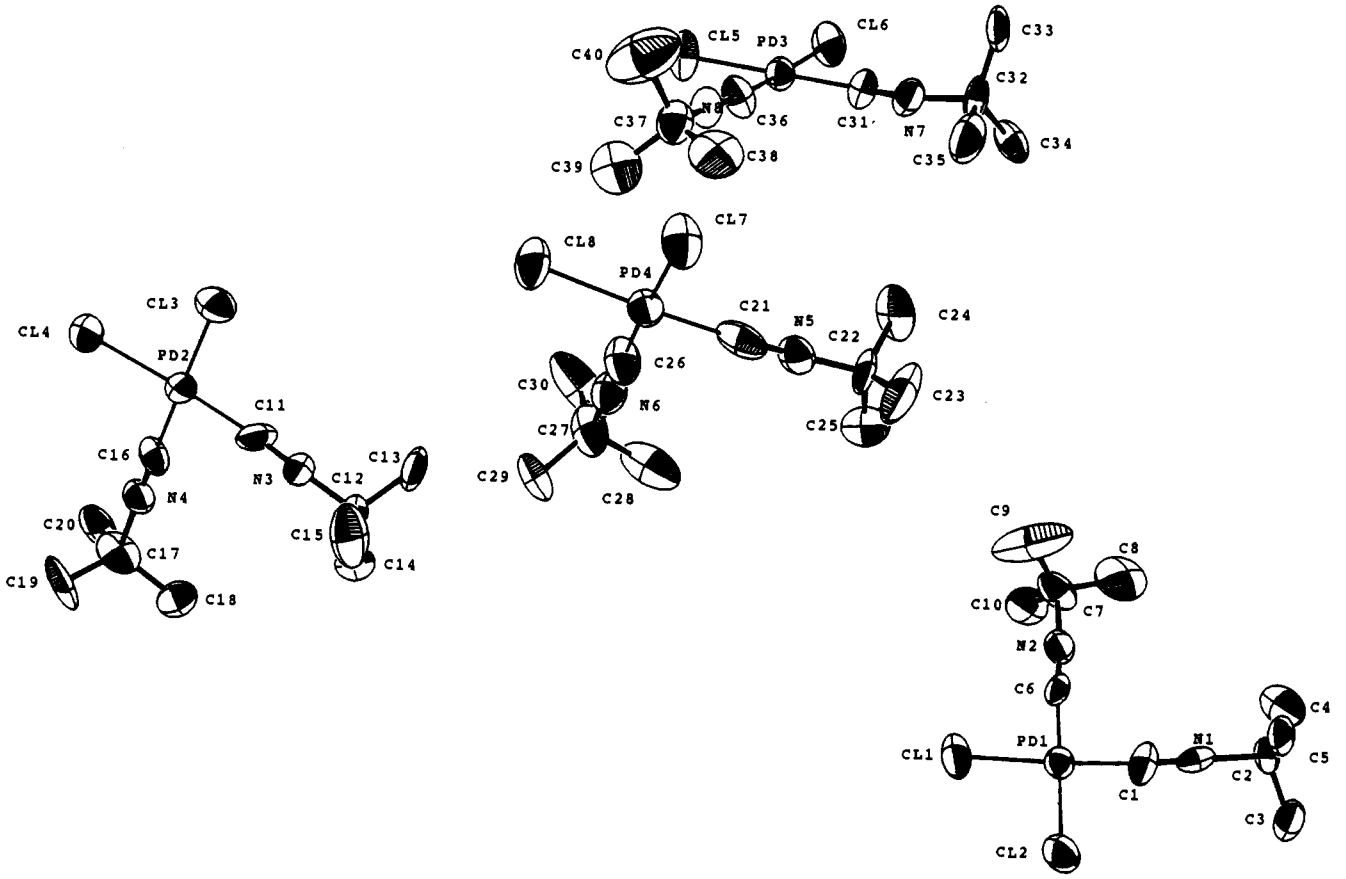

Figure 4. Molecular structure and atom labeling for the *cis*-$Pd(CNC(CH_3)_3)_2Cl_2$ complexes. The ORTEP[17c] drawing is shown with 50% probability ellipsoids.

Table IV. Selected Valence Angles (deg) for $Ag_2(dmb)_2X_2$ Complexes (X = Cl, Br, I)

$Ag_2(dmb)_2Cl_2$		$Ag_2(dmb)_2Br_2$		$Ag_2(dmb)_2I_2$	
Cl(1)–Ag–Cl(1)a	100.60(9)	Br(1)–Ag(1)–Br(2)	106.54(10)	I–Ag–I(a)	109.29(3)
Ag–Cl(1)–Ag(a)	79.40(8)	Br(1)–Ag(2)–Br(2)	105.45(10)	Ag–I–Ag(a)	70.71(3)
Ag–C(1)–N(1)	168.1(9)	Ag(1)–Br(1)–Ag(2)	74.69(9)	Ag–C(1)–N(1)	162.8(8)
Ag–C(9)–N(2)	164.8(9)	Ag(1)–Br(2)–Ag(2)	72.38(8)	Ag–C(9)–N(2)	162.9(8)
C(1)–Ag–C(9)	149.6(4)	Ag(1)–C(1)–N(1)	163.3(18)	C(1)–Ag–C(9)	146.3(4)
Cl(1)–Ag–C(1)	100.0(3)	Ag(2)–C(9)–N(2)	160.8(18)	I–Ag–C(1)	98.6(2)
Cl(1)–Ag–C(9)	99.0(3)	Ag(2)–C(13)–N(3)	162.4(19)	I–Ag–C(9)	100.2(3)
Cl(1)a–Ag–C(1)	100.0(3)	Ag(1)–C(21)–N(4)	161.8(18)	I(a)–Ag–C(1)	98.6(2)
Cl(1)a–Ag–C(9)	98.8(3)	C(9)–Ag(2)–C(13)	147.0(8)	I(a)–Ag–C(9)	98.6(2)
		C(1)–Ag(1)–C(21)	142.9(8)		
		Br(1)–Ag(1)–C(1)	102.1(5)		
		Br(1)–Ag(1)–C(21)	107.8(6)		
		Br(2)–Ag(1)–C(1)	91.4(5)		
		Br(2)–Ag(1)–C(21)	100.5(6)		
		Br(1)–Ag(2)–C(9)	99.4(6)		
		Br(1)–Ag(2)–C(13)	107.0(6)		
		Br(2)–Ag(2)–C(9)	94.5(6)		
		Br(2)–Ag(2)–C(13)	97.2(6)		

(3.452(2) Å, X = Cl; 3.347(3) Å, X = Br; 3.379(2) Å, X = I) are longer than the one found in a structurally related $Rh_2(dmb)_2(dppm)_2^{2+}$ complex[19] ($r(Rh_2)$ = 3.101(2) Å) and are at the limit of the sum of the van der Waals radii (3.40 Å),[19] indicating that weak metal–metal interactions occur. The $r(Ag_2)$ value for the bromo derivative deviates slightly from the other ones; this difference could be associated with the "butterfly" structure of the complex. Each tetracoordinated silver atom exhibits a distorted tetrahedral structure, where the X–Ag–X and C–Ag–C angles average 100.60(9) and 149.6(4), 106.0(5) and 145(2), and 109.29(3) and 146.3(4)°, for X = Cl, Br, and I, respectively (see Tables II and III for selected bond distances and bond angles). The average r(Ag–X) values are 2.70(2), 2.80(2), and 2.920(15) Å for X = Cl, Br, and I, respectively and indicate that the Ag–X bonds prossess significant ionic character.[20] However, the Ag–X bonding interactions are much less ionic than those found in the structurally related $Au_2(dmpm)_2Cl_2$ complex, where the Au–Cl distances (3.462(2) and 3.519(3) Å) are greater than the sum of the ionic radii in this case ($r_{ion}(Au^+)$ = 1.51 Å).[19] The Ag–X–Ag angles are 79.40(8), 74.69(9) and 72.38(8), and 70.71(3)° for X = Cl, Br, and I, respectively, and are smaller than the one found in the intermolecular Ag–(μ-Br)$_2$–Ag bridge (86.94(4)°)[1] for $Ag_2(dmpm)_2Br_2$, and the 90° angle between two p orbitals. The large deviation of the C–Ag–C angle from that of a normal two-

(19) Boyd, D. C.; Matsch, P. A.; Mixa, M. M.; Mann, K. R. *Inorg. Chem.* **1986**, *19*, 3331.

(20) (a) See: Cotton, F. A.; Wilkinson, G.; Gauss, P. L. *Basic Inorganic Chemistry*, 2nd ed.; Wiley: Toronto, 1987; p 60. (b) The ionic radii (r_{ion}) for Ag^+, Cl^-, Br^-, and I^- are 1.08, 1.67, 1.82 and 2.06 Å, respectively. The covalent radii (r_{cov}) for Ag, Cl, Br, and I are 1.44, 0.99, 1.14, and 1.33, respectively.[20a]

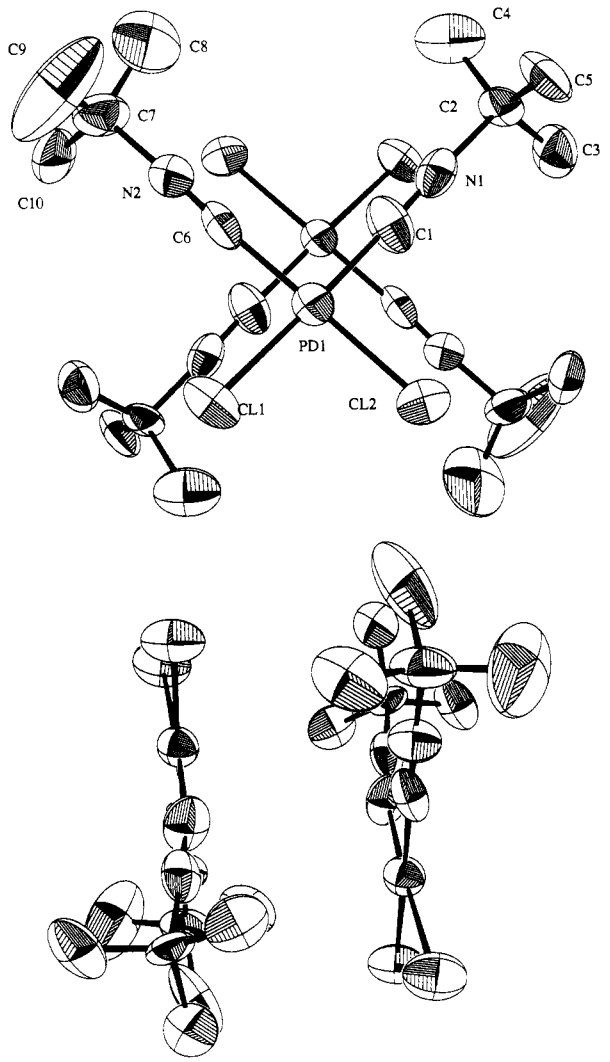

Figure 5. Front and side views of a *cis*-Pd(CNC(CH$_3$)$_2$Cl$_2$ dimer. The ORTEP[17c] drawing is shown with 50% probability ellipsoids.

coordinate structure (180°) strongly suggests that the Ag–X interactions are important. In the $Ag_2(dmpm)_2Br_2$[1] and [Ag(CN-2,6-((CH$_3$)$_3$C)$_2$C$_6$H$_3$)$_2$(PF$_6$)][21] complexes, the Ag–X distances are 2.7431(13) and 2.9453(13) Å (X = Br) and 2.668(14) Å (X = F from PF_6^-), respectively. The Ag–C (2.10 < *r*(Ag–C) < 2.18 Å) and other bond distances and angles are all normal (Tables III and IV). The dmb ligands are disordered, but the molecules lie on a center of symmetry suggesting that the molecules belong to the C_{2h} point group.

The chloro and iodo derivatives crystallize with two chloroform molecules and with one ethanol molecules respectively and are very sensitive to drying. The shortest distances observed are 3.353(16) Å between the C(13) (of the acidic chloroform molecules) and the Cl(1) atoms in $Ag_2(dmb)_2Cl_2$ (C(13)–H–Cl(1) angle = 160.1(7)° and 3.96(3) Å between the O (ethanol) and I atoms in $Ag_2(dmb)_2I_2$. In the former case, H-bonding may be the origin of these interactions.

The Pd(CNC(CH$_3$)$_3$)$_2$Cl$_2$ structure shows the expected square planar geometry for the cis configuration.[22] The compound crystallizes in the P$\bar{1}$ space group (Z = 8), where the formation of quasi-face-to-face dimers occur (Figures 4 and 5). Four independent dimers are observed, where the Pd–Pd separations

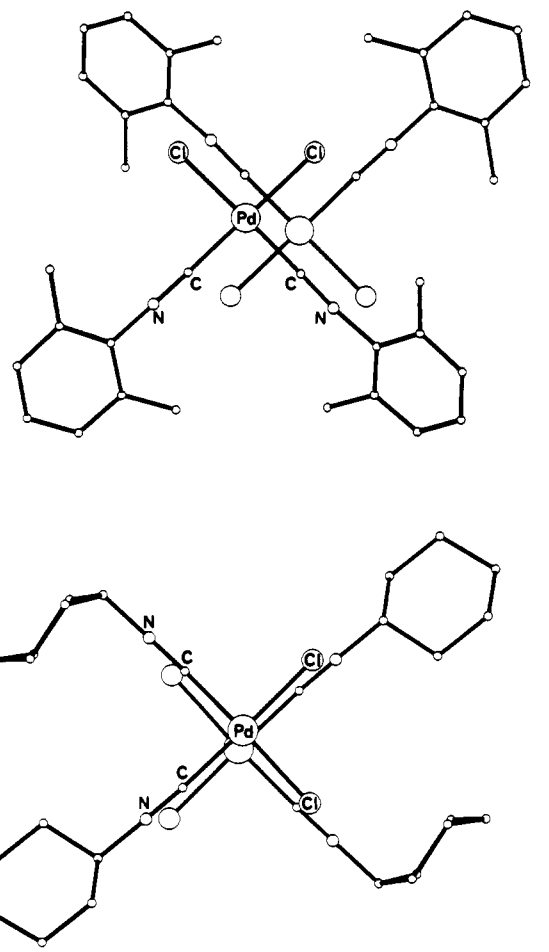

Figure 6. Molecular structure of the *cis*-Pd(CNR)$_2$Cl$_2$ dimers: R = 2,6-(CH$_3$)$_2$C$_6$H$_3$ (top); R = C$_6$H$_{11}$ (bottom).

are 4.441(3) Å (Pd(1)–Pd(1)), 4.359(3) Å (Pd(2)–Pd(2)), 4.056(3) Å (Pd(3)–Pd(3)), and 4.463(3) Å (Pd(4)–Pd(4)). In the cases where the isocyanide ligands were xylenyl- and cyclohexylisocyanides, the X-ray structures revealed C_{2h} symmetry dimers where the Pd–Pd contacts were 4.061(2) and 3.593(2) Å, respectively (Figure 6). Intermolecular steric hindrance between the *tert*-butyl groups and crystal packing are very likely at the origin of nonperfectly oriented face-to-face structure in this case. Nonetheless, very weak Pd–Pd interactions (a series of three averaging 4.42(6) Å and one at ~4.06 Å) are expected in the solid state.

Low-Frequency Vibrational Spectra. The 400–4000-cm^{-1} region is the mono- and diisocyanide (diphenyltriazide and trifluoroacetate) ligand fingerprint, and very few changes are observed upon complexation with the metal atoms; this region has not been investigated in this work. The lower frequency region is analyzed using assignments made by different research groups for complexes of the type $M_2(dppm)_2X_2$,[23] $Ag_2(dmpm)_2Br_2$,[1] $Au_2(ylid)_2X_2$[24] (ylid = $(CH_2)_2P(C_6H_5)_2$), and $[M_2(CNCH_3)_6](PF_6)_2$[25] (M = Pd, Pt; X = Cl, Br, I).

Figures 7–9 show the vibrational spectra (10–400 cm^{-1}) for the solid $Ag_2(dmb)_2X_2$ complexes (X = Cl, Br, I). Two sets of Raman spectra are presented where two laser excitations were used: 488.0 nm (microRaman) and 1064 nm (FT-Raman). The vibrational data are the same except that the FT-Raman spectra are more informative in the 80–400-cm^{-1} region, while the microRaman spectra provide data below 80 cm^{-1}.[26] The vibra-

(21) Yamamoto, Y.; Aoki, K.; Yamazaki, H. *Inorg. Chim. Acta* **1982**, *68*, 75.

(22) The average Pd—Cl (2.29(1) Å), Pd—C(1.93(5) Å), and C≡N (1.14(2) Å) bond distances are all normal. The average Cl—Pd—Cl, C—Pd—C, and Pd—C≡N bond angles are 93.0(8), 90(1), and 175(3)°, respectively. Details of the molecular structure are provided in the supplementary material.

(23) Alves, O. L.; Virtoge, M.-C.; Sourisseau, C. *Nouv. J. Chim.* **1983**, *7*, 231.

(24) Clark, R. J. H.; Tocker, J. H.; Fackler, J. P., Jr.; Neira, R.; Murray, H. H.; Knackel, H. *J. Organomet. Chem.* **1986**, *303*, 437.

(25) Garciafigueroa, E.; Sourisseau, C. *Nouv. J. Chim.* **1978**, *2*, 593.

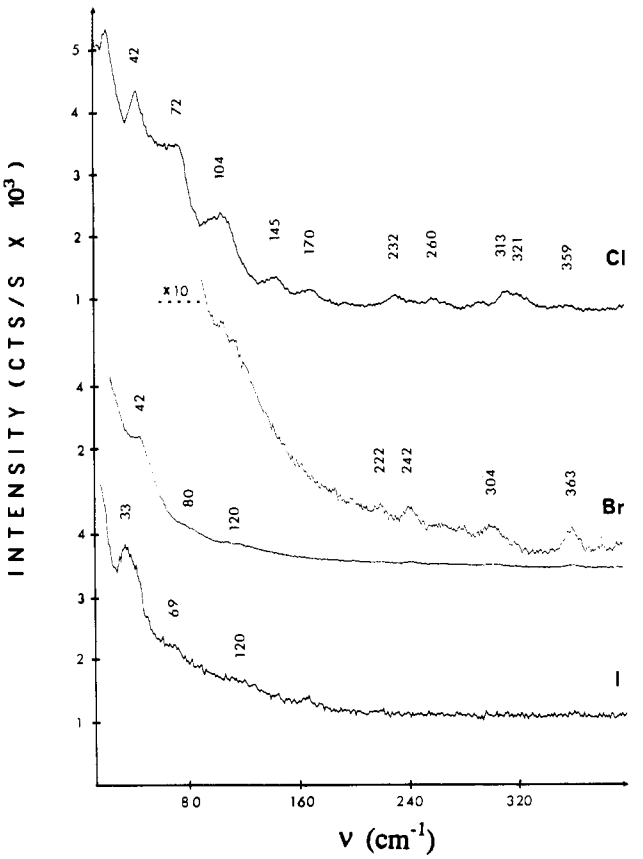

Figure 7. Micro-Raman spectra (10–400 cm^{-1}) of solid $Ag_2(dmb)_2X_2$ complexes (X = Cl, Br, I). Experimental conditions: laser excitation, 488.0 nm; laser power, 5–10 mW at the sample; 300-μm slits; 2s/point at every 1 cm^{-1}; 32 × objective; one scan.

Table V. Low-Frequency Vibrational Data (cm^{-1}) for $Ag_2(dmb)_2X_2$ Complexes (X = Cl, Br, I)

$Ag_2(dmb)_2Cl_2$		$Ag_2(dmb)_2Br_2$		$Ag_2(dmb)_2I_2$		
Raman	IR	Raman	IR	Raman	IR	assignments
42		42		33		ν(M–M)
72		84		69		δ(CMC)
104	125					ν(M–X)
145	155	120	107		107	ν(M–X)
170	~175 sh	139	135	119	120	ν(M–X)
		189		175		skeleton deformations
		222		215		skeleton deformations
232		242		~240		skeleton deformations
260		270		268		skeleton deformations
301	308	298	306	300	305	δ(MCN)
313						δ(MCN)
321		320		322		δ(MCN)
359	360	362	362	364	365	ν(AgC)
		380		383		ν(AgC)
399		396		398		ν(AgC)

tional mode of interest in this work is $\nu(M_2)$. This mode generally dominates the Raman spectra, and on the basis of the frequency range where this mode should appear (see Table V for examples), $\nu(M)_2$ is assigned at 42, 42, and 33 cm^{-1} for X = Cl, Br, and I, respectively. The 42-cm^{-1} value compares favorably with the ones found in the $Ag_2(dmpm)_2Br_2$ complex (48 cm^{-1})[1] and in the heavier $Au_2(dmb)(CN)_2$ complex (36 cm^{-1}).[1] Interestingly, the

(26) (a) The possibility of preresonance enhancement in the 488.0-nm irradiation spectra could be the origin of the difference in the interpeak intensity ratio between the 488- and 1064-nm spectra. The $Ag_2(dmb)_2X_2$ complexes (X = Cl, Br, I) absorb in the 200–250-nm region and are phosphorescent between 400 and 500 nm. (b) The FT-Raman spectrometer uses a notch filter that cuts off the laser excitation (cutoff ~ 60–70 cm^{-1}); information below this limit is not available. The combination of both techniques affords a much better analysis of the spectra.

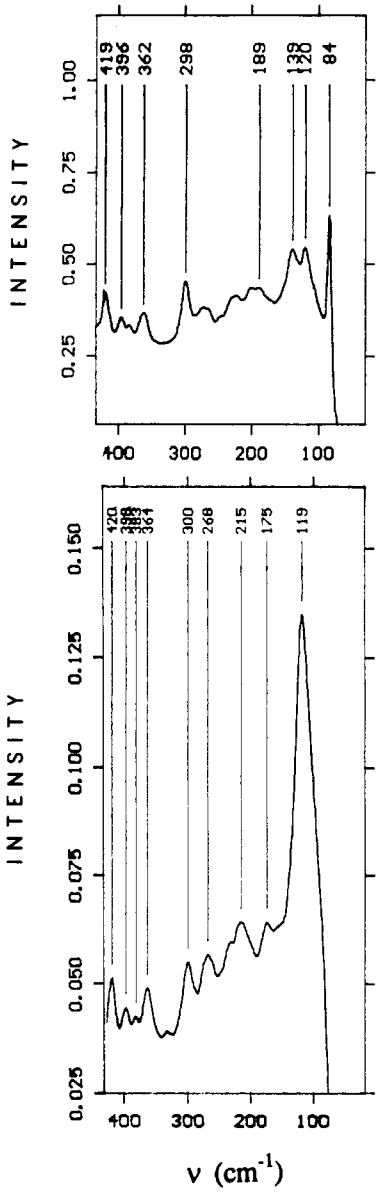

Figure 8. FT-Raman spectra (70–430 cm^{-1}) of the solid $Ag_2(dmb)_2X_2$ complexes (X = Br, I). Experimental conditions: laser excitation, 1064 nm; laser power, ~160 mW; resolution, 4 cm^{-1}; focused; 100 scans.

$\nu(Ag_2)$ data are sensitively greater than that for the Cd_2 species in the gas phase ($r(Cd_2)$ = 3.3 ± 0.1, 3.05 ± 0.15, 3.0 ± 0.1 Å; $\nu(Cd_2)$ = 21, 37, and 39 cm^{-1} for the $^1\Sigma_g^+$, $^3\Sigma_u^+$ and $^1\Sigma_u^+$ electronic states, respectively),[27] indicating that the Ag–Ag interactions are stronger than those for the Cd_2 systems, which is consistent with the fact that $r_{vdW}(Ag) > r_{vdW}(Cd)$.

The ν(AgX) bands are quickly identified in the far-IR spectra (Figure 9) as being the broadest and most intense in the 80–400-cm^{-1} region. The Raman-active ν(AgX) bands are assigned on the basis of the frequency range where they should be observed according to the literature data. As expected, ν(AgX) decreases with X masses. The local symmetry for the Ag_2X_2 unit is D_{2h}, where four ν(AgX) modes are predicted ($a_g + b_{1g} + b_{2u} + b_{3u}$). For M_2L_6 complexes, almost systematically $\nu(a_g) > \nu(b_{1g})$.[28] On the basis of this observation, we assign the a_g modes at 170, 139, and 119 cm^{-1} for X = Cl, Br, and I, respectively, placing the b_{1g} modes at 145 and 120 cm^{-1} for X = Cl and Br, respectively. For the $Ag_2(dmb)_2I_2$ complex, the 119-cm^{-1} scattering is relatively intense and broad; both the a_g and b_{1g} modes may very well be accidently degenerate under this broad envelope. Ignoring the perpendicularly oriented isocyanide

(27) Bousquet, C. *J. Phys. B: Mol. Phys.* **1987**, *20*, 2217.

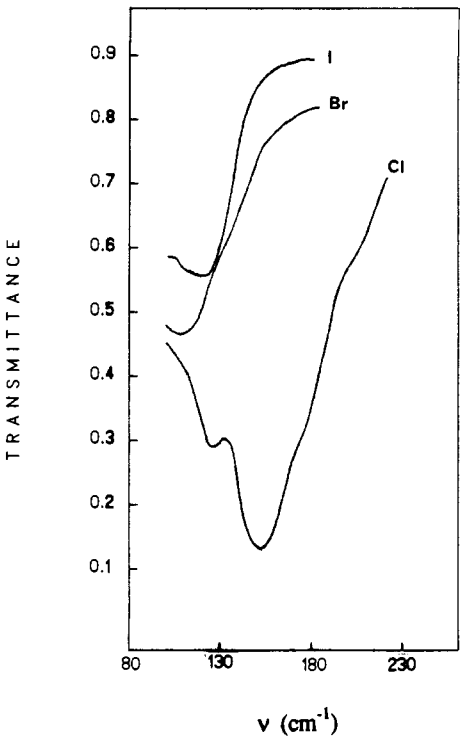

Figure 9. Far-IR spectra (100–200 cm^{-1}) of the solid $Ag_2(dmb)_2X_2$ complexes (X = Cl, Br, I). Experimental conditions: resolutions, 4 cm^{-1}; 200 scans.

groups, the AgX force constant (F(AgX)) can be estimated using normal mode calculations[29]

$$\lambda(b_{1g}) = \frac{2F(MX)\,(\sin(\alpha/2) + (M_M/M_X)\cos^2(\alpha/2)/\sin(\alpha/2))^2}{M_M(1 + (M_M/M_X)\cot^2(\alpha/2))} \quad (1)$$

where M_M and M_X are the metal and halogen masses, α is the XMX angle, and λ is $4\pi^2c^2\nu^2$. Using the crystallographic data from Table IV (α = 100.6, 106.0 (average value), and 109.3° for X = Cl, Br, and I, respectively), we obtain F(AgX) = 0.37, 0.41, and 0.47 mdyn $Å^{-1}$, respectively. These values are small and are consistent with the relatively long AgX bonds.[30] However the increase in F(AgX) with the row number suggests that the AgX bond becomes somewhat stronger in going from X = Cl to I.[31]

The $Ag_2(C_6H_5N_3C_6H_5)_2$ Raman spectrum (Figure 10) is also characterized by a medium intense $\nu(Ag_2)$ band (i.e. at 114 cm^{-1}).

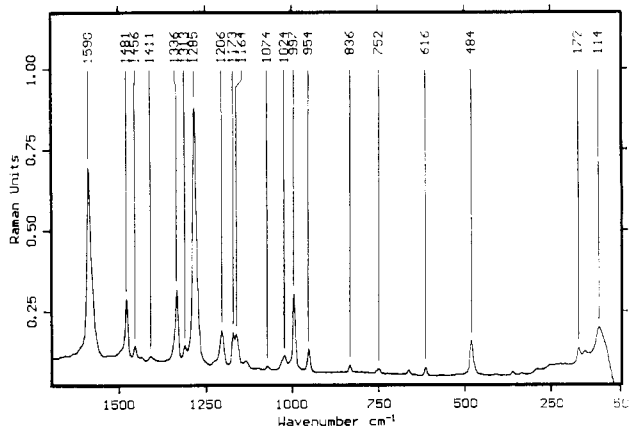

Figure 10. FT-Raman spectra (70–1600 cm^{-1}) of solid $Ag_2(C_6H_5NNNC_6H_5)_2$. Experimental conditions are identical to those for Figure 4, except laser power was 70 mW.

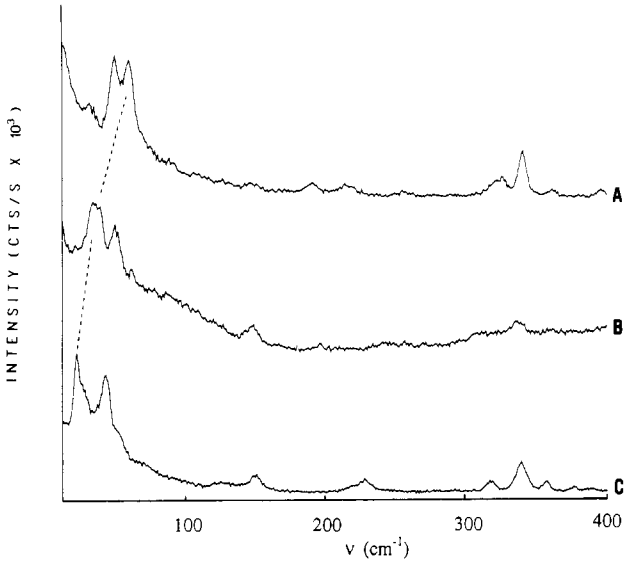

Figure 11. Micro-Raman spectra (10–400 cm^{-1}) of the solid *cis*-$Pd(CNR)_2Cl_2$: (A) R = C_6H_{11}; (B) R = 2,6-$(CH_3)_2C_6H_3$; (C) R = $(CH_3)_3C$. Experimental conditions are identical to those for Figure 3.

The higher frequency of this mode is consistent with the shorter $r(Ag_2)$ value (2.669 Å).[14] The ν(AgN) band is located at 483 cm^{-1}.[32] The $\nu(Ag_2)$ band in the $Ag_2(CF_3CO_2)_2$ spectra does not appear as a well-resolved peak, but rather as a shoulder (~80 cm^{-1}; $r(Ag_2)$ = 2.967 Å). This behavior is not uncommon for Ag_2 systems[1] (see also the spectrum for $Ag_2(dmb)_2Br_2$). The ν(AgO) band is observed at 458 cm^{-1}.[32]

The Raman spectra for the solid *cis*-$Pd(CNR)_2Cl_2$ complexes are shown in Figure 11, and are characterized by two intense scatterings below 60 cm^{-1} (i.e. in the lattice region); the $\nu(Pd_2)$ bands are expected to appear in this range. Knowing that $\nu(Pd_2)$ is sensitive to $r(Pd_2)$, we associate the shifting peak from 58 to 32 and to 19 cm^{-1} for R = C_6H_{11}, 2,6-$(CH_3)_2C_6H_3$, and $(CH_3)_3C$, (where r(Pd–Pd) = 3.593, 4.061 and 4.42(6) Å), respectively, with Pd–Pd motions. These ν values compare favorably with those for $[Rh(CNC_6H_5)_4]_2^{2+}$ ($\nu(Rh_2)$ = 60, $r(Rh_2)$ = 3.193)[33,34] and for $Rh_2(dmb)_4^{2+}$ ($\nu(Rh_2)$ = 26 cm^{-1}, $r(Rh_2)$ = 4.4 Å)[35] and

(28) (a) Nakamoto, K. *Infrared and Raman Spectra of Inorganic and Coordination Compounds*, 4th ed.; Wiley: New York, 1986; p 161. (b) Adams, D. M.; Churchil, R. G. *J. Chem. Soc. A* **1968**, 2141. (c) Goggin, P. L. *J. Chem. Soc., Dalton Trans.* **1974**, 1483. (d) Adams, D. M.; Churchil, R. G. *J. Chem. Soc. A* **1970**, 697. (e) See also: Beattie, I. R.; Gilson, T. R.; Ozin, G. A. *J. Chem. Soc. A* **1968**, 2765. (f) Forneris, R.; Hiraishi, J.; Miller, F. A.; Vehara, M. *Spectrochim. Acta* **1970**, *26A*, 581.

(29) The equations for the normal mode calculations in M_2X_2 (D_{2h}) systems were kindly provided by Dr. V. M. Miskowski (unpublished results). Equations for the normal mode calculations in cyclobutane, cyclobutadiene and cyclobutanedione are also known: Trenkler, F. *Proc. Indian Acad. Sci., Sect. A* **1938**, *8*, 383.

(30) (a) For comparison, the AgX distances in the solid AgX compounds are 2.48, 2.63, and 2.87 Å for X = Cl, Br, and I, respectively.[30b] These AgX interactions are considered to be strong. Incidentally the corresponding ν(AgX) are 343.6, 247.7, and 206.2 cm^{-1} for X = Cl, Br, and I, respectively (see ref 28, p 104). (b) Huheey, J. E. *Inorganic Chemistry; Principles of Structure and Reactivity*; 3rd ed.; Harper & Row: New York, 1983; p 73.

(31) This trend is consistent with the relative gain in covalent character and the loss in relative ionic character in the AgX bonds, going from X = Cl to I, in the particular system. This behavior can be quantified using the following equations: $\Delta = [r_{ion}(Ag^+) + r_{ion}(X^-)] - r_{obs}(AgX)$ for the loss in ionic character, and $\Delta' = [r_{cov}(Ag) + r_{cov}(Cl)] - r_{obs}(AgX)$ for the gain in covalent character. See footnote 20 and Table II for data.

(32) The other observed Raman frequencies for $Ag_2((C_6H_5)NNN(C_6H_5))_2$ (96, 155, 172, 214, 226, 254, 293, 340, 366, 393, 411, and 442 cm^{-1}) and $Ag_2(CF_3CO_2)_2$ (39, 130, 150, 192, and 287 cm^{-1}) are not interpreted in this work. Far-IR data for $Ag_2(CF_3CO_2)_2$: 457, 315, 283, 193, 159, 125, and 61 cm^{-1}.

(33) Dallinger, R. F.; Miskowski, V. M.; Gray, H. B.; Woodruff, W. H. *J. Am. Chem. Soc.* **1981**, *103*, 1595.

(34) Mann, K. R.; Lewis, N. S.; Williams, R. M.; Gray, H. B.; Gordon, J. G., II *Inorg. Chem.* **1978**, *17*, 828.

(35) Miskowski, V. M. Unpublished results.

Table VI. Spectroscopic and Structural Data for Very Weakly Interacting Metallic Dimers

	$\nu(M_2)$, cm^{-1}	$F(M_2)$, mdyn $Å^{-1}$ [a]	$r(M_2)$, Å	$2r_{vdw}$, Å[b]
$Ag_2(dmb)_2Cl_2$	42[c]	0.056	3.451[c]	3.40
$Ag_2(dmb)_2Br_2$	42[c]	0.056	3.345[c]	3.40
$Ag_2(dmb)_2I_2$	33[c]	0.035	3.378[c]	3.40
$Ag_2(dmpm)_2Br_2$	48[d]	*e*	3.601[d]	3.40
$Au_2(dmb)(CN)_2$	36[d]	0.075	3.536[f]	3.40
[*cis*-$Pd(CNC_6H_{11})_2Cl_2]_2$	58[c]	0.106	3.593[g]	3.20
[*cis*-$Pd(CN\text{-}2,6\text{-}(CH_3)_2C_6H_3)_2Cl_2]_2$	32[c]	0.032	4.061[h]	3.20
[*cis*-$Pd(CNC(CH_3)_3)_2Cl_2]_2$	19[c]	0.011	4.42[c]	3.20
$[Rh(CNC_6H_5)_4]_2^{2+}$	60[i]	0.109	3.193[j]	
$Mg_2(^1\Sigma_g^+)$	51.12[k]	0.019	3.89[k]	3.40
$Ca_2(^1\Sigma_g^+)$	64.92[k]	0.050	4.28[k]	
$Ca_2(^1\Sigma_g^+)$	42.02[k]	0.069	4.47[k]	
$Cd_2(^1\Sigma_g^+)$	21[l]	0.015	3.31[l]	3.20
$Cd_2(^3\Sigma_u^+)$	37[l]	0.045	3.05[l]	3.20
$Cd_2(^1\Sigma_u^+)$	39[l]	0.050	3.0[l]	3.20
$Hg_2(^1\Sigma_g^+)$	18.5[m]	0.020	3.63[m]	3.00
$Hg_2(^1\Sigma_u^+)$	19.7[m]	0.023	3.61[m]	3.00

[a] $F(M_2) = \mu(2\pi c\nu(M_2))$,[2] unless stated otherwise. [b] $2r_{vdW}$ = sum of the van der Waals radii; from ref 22. [c] From this work. [d] From ref 1. [e] Estimated to be ~0.03 mdyn $Å^{-1}$. [f] Che, C.-M.; Wong, W.-T.; Lai, T.-F.; Kwong, H.-L. *J. Chem. Soc., Chem. Commun.* **1989**, 243. [g] From ref 12. [h] From ref 13. [i] From ref 33. [j] From ref 34. [k] Huber, K. P.; Herzberg, G. *Molecular Spectra and Molecular Structure Constants of Diatomic Molecules*; Va Nostrand: New York, 1979. [l] From ref 27. [m] Van Zee, R. D.; Blankespoor, S. C.; Zwier, T. S. *J. Chem. Phys.* **1988**, *88*, 4650.

Table VII. Low-Frequency Raman Data for *cis*-$Pd(CNR)_2Cl_2$ Complexes[a]

R = C_6H_{11}	R = 2,6-$(CH_3)_2C_6H_3$	R = $(CH_3)_3C$	assignments
		19	ν(Pd–Pd)
		30	ν(Pd–Pd)
30		40	$\nu_{lattice}$
48	47	46 sh	$\nu_{lattice}$
58	32		ν(Pd–Pd)
	58 w	61 sh	
	~100 v br	~80 sh	
		120 sh	
145	147	148	π(ClPdCl), δ(C–Pd–C) + other skeleton motions
190	194		π(ClPdCl), δ(C–Pd–C) + other skeleton motions
217		217	π(ClPdCl), δ(C–Pd–C) + other skeleton motions
254	240	226	
325	315	318	ν(PdCl)
340	336	339	ν(PdCl)
361		356	ν(PdC)
361		376	ν(PdC)

[a] π = out-of-plane deformation; δ = in-plane deformation.

are unambiguously assigned to $\nu(Pd_2)$. We also note that there is a weaker shoulder at ~30 cm^{-1} in the *cis*-$Pd(CNC(CH_3)_3)_2Cl_2$ spectrum; this band is also assigned to $\nu(Pd_2)$ accounting for the Pd(3)–Pd(3) dimer (r(Pd–Pd) = 4.06 Å). The second strong band (47 ± 1 cm^{-1}), which is weakly sensitive to the nature of the R groups is also assigned to a lattice mode in agreement with the Raman datum reported for $[Pd(CNCH_3)_4](PF_6)_2$ (ν = 45 cm^{-1}; very intense).[25] The dimeric forms are not retained in solution, so polarization measurements were not possible.

The $\nu(M_2)$ bands (assigned primarily on the basis of their strong intensities in the Raman spectra and by comparison with well-known compounds) compare favorably with those for van der Waals bimetallic molecules (see Table VI for details). The M_2 interactions are obviously weak, but not negligible. Typically, the $F(M_2)$ values associated with a formal M–M single bond are ~1.2 to 1.3 mdyn $Å^{-1}$ for Ag_2 and Pd_2 systems. At the $2r_{vdw}$ critical limits, the samples exhibiting such M–M separations show $F(M_2)$ of ~0.05 mdyn $Å^{-1}$ (for Ag_2) and ~0.18 mdyn $Å^{-1}$ (for Pd_2) which represent essentially ~$^1/_{20}$ and ~$^1/_7$ of single Ag–Ag and Pd–Pd bonds, respectively.

Table VIII. Structural and Spectroscopic Data for Ag_2 Compounds

	$\nu(Ag_2)$, cm^{-1}	$F(Ag_2)$, mdyn $Å^{-1}$ [a]	$r(Ag_2)$, Å	Woodruff's $r(Ag_2)$, Å[b]
$Ag_2(dmpm)_2Br_2$	48[c]		3.601(2)[c]	3.28
$Ag_2(dmb)_2I_2$	33[d]	0.034	3.378(2)[d]	3.26
$Ag_2(dmb)_2Cl_2$	42[d]	0.056	3.451(2)[d]	3.25
$Ag_2(dmb)_2Br_2$	42[d]	0.056	3.345(1)[d]	3.25
$[Ag_2(dppm)_3](PF_6)_2$	76[c]	0.18	3.10(1)[e]	3.18
$[Ag_2(dmpm)_2](PF_6)_2$	76[c]	0.18	3.041(1)[f]	3.18
$Ag_2(O_2CCF_3)_2$	80[d]	0.20	2.967(3)[g]	3.17
$Ag_2(C_6H_5NNNC_6H_5)_2$	114[d]	0.41	2.669(1)[h]	3.07
Ag_3	120.5[i]			
$Ag_2^-(^2\Sigma_u^+)$	118[j]	0.44	2.814[j]	3.05
$Ag_2(^1\Sigma_g^+)$	192.8[i]	1.18	2.471[j]	2.74

[a] $F(M_2) = \mu(2\pi c\nu(M_2))^2$, μ = reduced mass. [b] Calculated using eq 4. [c] From ref 1. [d] This work. [e] Average values for various $Ag_2(dppm)_2^{2+}$ complexes taken from ref 36a,b. [f] From ref 36c. [g] From ref 16. [h] From ref 14. [i] From ref 36d. [j] From ref 36e.

Table IX. Structural and Spectroscopic Data for Pd_2 Compounds

	$\nu(Pd_2)$, cm^{-1}	$F(Pd_2)$, mdyn $Å^{-1}$ [a]	$r(Pd_2)$, Å	Woodruff's $r(Pd_2)$, Å[b]
[*cis*-$Pd(CNC(CH_3)_3)_2Cl_2]_2$	19[c]	0.011	4.42(6)[c]	3.27
	~30[c]	~0.028	4.056(3)[c]	3.26
[*cis*-$Pd(CN\text{-}2,6\text{-}(CH_3)_2C_6H_3)Cl_2]_2$	32[c]	0.032	4.061(2)[d]	3.26
[*cis*-$Pd(CN\text{-}C_6H_{11})_2Cl_2]_2$	58[c]	0.106	3.593(2)[e]	3.22
$Pd_2(dba)_3$	76[f]	0.18	3.245(5)[g]	3.18
$Pd_2(dppm)_3$	120[h]	0.45	2.956(1)[i]	3.05
$Pd_2(^1\Sigma_g^+)$	132[j]	0.55	2.804[k]	3.00
$Pd_2(dppm)_2Br_2$	120[l]	0.75[m]	2.699(2)[m]	2.92
$Pd_2(dppm)_2Cl_2$	152[l]	1.15[m]	2.644(2)[n]	2.76
$Pd_3(CNCH_3)_8^{2+}$	140, 114[o]	1.26[q]	2.591(2)[r]	2.72
$Pd_2(CNCH_3)_6^{2+}$	160[s]	2.02[t]	2.531(1)[u]	2.53
Pd_3	230[v]	1.10[w]	2.70(3)[x]	2.78

[a] $F(M_2) = \mu(2\pi c\nu(M_2))^2$ (μ = reduced mass), unless stated otherwise. [b] Calculated using eq 4. [c] This work. [d] From ref 13. [e] From ref 12. [f] From ref 37a. [g] Average values taken from ref 37b,c. [h] From ref 37d. [i] From ref 37e. [k] Calculated datum from ref 37k. [l] From ref 23. [m] Calculated from the equations of X–M–M–X systems (Herzberg, G. *Molecular Spectra and Molecular Structure*; Van Nostrand: New York, 1945; Vol. II, p 180); the symmetric and asymmetric ν(MX) are 273 and 247 cm^{-1} and 213 and 189 cm^{-1} for X = Cl, and Br, respectively.[23] [n] From ref 37f. [o] Datum for $Pd_2(dppm)_2(SnCl_3)Cl$ where both $\nu(Pd_2)$ (147 cm^{-1}) and ν(PdCl) (274 cm^{-1}) are essentially unaffected when replacing the Cl atom by the $SnCl_3$ group.[23] The Raman active ν(PdCl) in $Pd_2(dppm)_2Cl_2$ is 273 cm^{-1}. [p] From ref 37h. [q] Calculated using equations for X–M–M–M–X systems and using the approximations outlined in Engler and Kohlrausch (Engler, W.; Kohlrausch, K. W. F. *Z. Phys. Chem.* **1936**, *34*, 214) using ν(Pd–CN) = 262 cm^{-1}.[37h] The quadratic solution provided two solutions, one of which is 3.92 mdyn $Å^{-1}$ and is physically unrealistic for a single Pd–Pd bond. This value is neglected in this work. [r] From ref 37i. [s] From ref 25. [t] Calculated from the equations of X–M–M–X systems using only the symmetric ν(Pd–CN) (294 cm^{-1}). [u] From ref 37j. [v] Measured for Pd_3^- by photoelectron spectroscopy from: Erwin, K. M.; Ho, J.; Lineberger, W. C. *J. Chem. Phys.* **1988**, *89*, 4514. [w] Calculated using $F = m(2\pi c\nu)^2/3$. [x] Average value between 2.67 and 2.733 Å calculated by a different theoretical method for a quasi-equilateral Pd_3 molecule from: Balasubramanian, K. *J. Chem. Phys.* **1989**, *91*, 307.

Discussion

Force Constants and Metal-Metal Separations. The comparison of the structural and spectroscopic data for the Ag_2 and Pd_2 compounds (including literature data)[36,37] are presented in Tables VIII and IX, respectively. In most cases, $F(M_2)$ has been estimated for X–M–M–X systems[38] using the diatomic approximation or normal mode calculations for non axially and axially substituted compounds, respectively. A plot of $r(M_2)$ (in Å) versus

(36) (a) Ho, D. M.; Bau, R. *Inorg. Chem.* **1983**, *22*, 4073. (b) Tiekink, E. R. T. *Acta Crystallogr.* **1990**, *C46*, 235. (c) Stendel, R. *Z. Naturforsch.* **1975**, *30B*, 281. (d) Schulze, W.; Becker, H. V.; Minkwitz, R.; Manzel, K. *Chem. Phys. Lett.* **1978**, *55*, 59. (e) Bauschlicher, C. S., Jr.; Langhoff, S. R.; Partridge, H. *J. Chem. Phys.* **1989**, *91*, 2412.

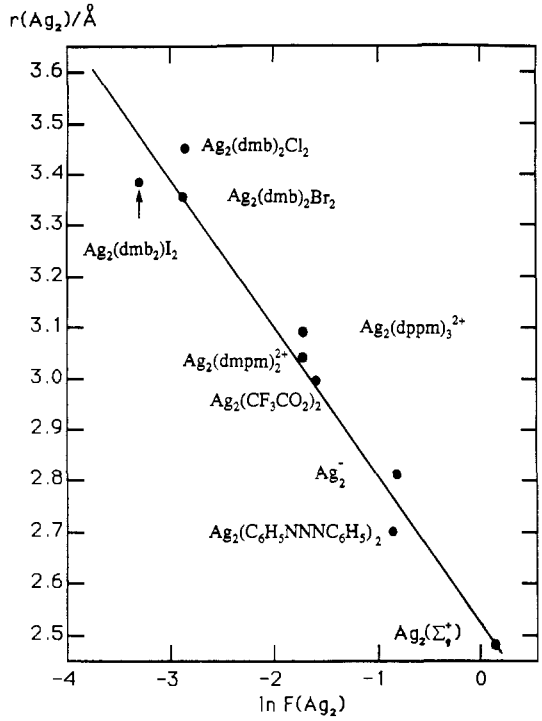

Figure 12. Graph of ln $F(Ag_2)$ vs $r(Ag_2)$.

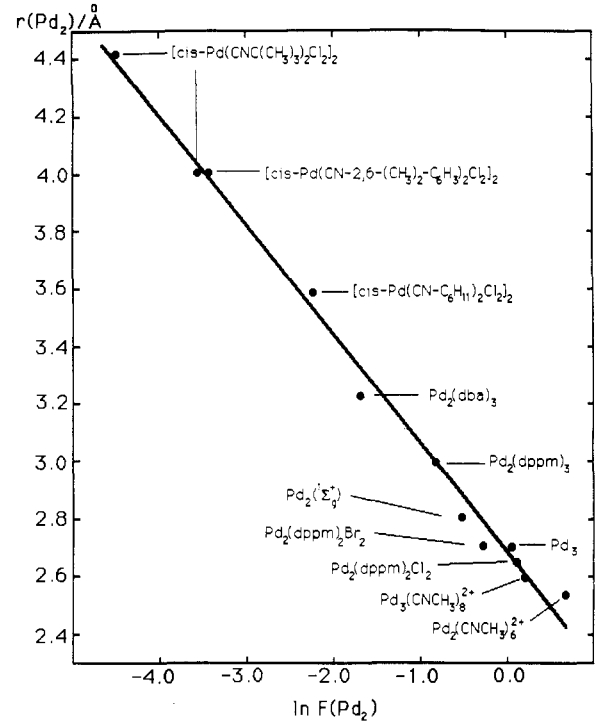

Figure 13. Graph of ln $F(Pd_2)$ vs $r(Pd_2)$.

ln $F(M_2)$ gives the reparametrized H–L relationships for Ag_2 and Pd_2 systems (Figures 12 and 13, respectively)

$$r(Ag_2) = -0.284(\ln F(Ag_2)) + 2.53 \quad (2)$$

$$r(Pd_2) = -0.387(\ln F(Pd_2)) + 2.67 \quad (3)$$

with correlation coefficients (σ) of 0.95 (9 data points) and 0.99 (12 data points) for the Ag_2 and Pd_2 systems, respectively. The comparison between $r(M_2)$ from eqs 2 and 3 and the experimental results is reasonably good (within 3%). The largest differences are found for the $Ag_2(dmb)_2X_2$ complexes (X = Cl, I) and $Pd_2(CNCH_3)_6^{2+}$ (between 3 and 4%). These larger differences are due to the difficulty in estimating $F(M_2)$.

For comparison purposes, the calculated $r(M_2)$ values from Woodruff's rules for the 4th row elements (eq 4)[4] are also examined (Tables VIII and IX):

$$r(4d) = 1.82 + 1.46(\exp(-F/2.61)) \quad (4)$$

The calculated $r(M_2)$ values compare surprisingly poorly with the experimental data with some exceptions in the Pd_2 systems. This phenomenon has been observed previously for Au_2 (and Ag_2) systems[1] and was attributed to the fact that these equations (Woodruff's rules)[4] become inadequate for $r(M_2) > 3.28$ Å (in the 4d row elements) and that they have been designed using data from homonuclear systems belonging to one particular row ignoring each individual behavior.[1]

The reparametrized H–L equation applied to Au_2 systems is[1]

$$r(Au_2) = -0.290(\ln F(Au_2)) + 2.68 \quad (5)$$

Two important features are observed: these relationships exhibit linearity above the sum of the van der Waals radii, and both slopes and intercepts are element-dependent. The first observation essentially questions the definition of r_{vdw} for the transition elements. Classically, the van der Waals model is a spherical one, and does not take into account the directional situation of the d–d orbital interactions in the M-M bonding. The second observation explains the apparent improved "accuracy" in relating $r(M_2)$ and $F(M_2)$ for the reparametrized H–L equations. The comparison of the slopes (m) and intercepts (b) are interesting; we find that going from eq 2 to eq 5 (Ag down to Au), m does not greatly change, while b increases. The m values could be intuitively explained by the fact that both elements belong to the same IB family of the periodic table. The b values could be explained, in part, by the fact that, to obtain similar $F(M_2)$ values, $r(M_2)$ should be larger for Au_2 simply because Au is heavier. A second factor to this are the r_{vdW} values (which do not apply in this comparison). The comparison of eqs 2 and 3 ($m(Pd_2) > m(Ag_2)$) indicates that the Pd–Pd interactions are more sensitive than the Ag–Ag ones in terms of distances. We cannot adequately correlate this empirical parameter with any property related to the elements at this time. For such a comparison, a systematic study of the periodic table is needed.

Acknowledgment. This research was supported by the NSERC and the FCAR. D.P. thanks the Université de Sherbrooke for an institutional graduate fellowship. P.D.H. thanks Professor I. S. Butler (McGill University) for providing access to the Raman Instruments, Mr. Y. Huang (McGill University) and Mrs. J. Hellman (Bruker) for technical assistance in the measurement of the Raman spectra, and Dr. V. M. Miskowski (Beckman Institute) for kindly providing the normal mode equations.

Supplementary Material Available: Tables giving crystal data and details of the structure determination, atomic coordinates, bond distances, bond angles, anisotropic thermal parameters, and hydrogen atom positions for the $Ag_2(dmb)_2X_2$ (X = Cl, Br, I) and *cis*-$Pd(CNC(CH_3)_3)_2Cl_2$ complexes (23 pages). Ordering information is given on any current masthead page.

(37) (a) Harvey, P. D.; Adar, F.; Gray, H. B. *J. Am. Chem. Soc.* **1989**, *111*, 1312. (b) Mazza, M. C.; Pierpont, C. G. *J. Chem. Soc., Chem. Commun.* **1973**, 207. (c) Ukai, T.; Kawazura, H.; Ishii, Y.; Bonnet, J.-J.; Ibers, J. A. *J. Organomet. Chem.* **1974**, *65*, 253. (d) Harvey, P. D.; Gray, H. B. *J. Am. Chem. Soc.* **1988**, *110*, 2145. (e) Kirss, R. V.; Eisenberg, R. *Inorg. Chem.* **1989**, *28*, 3372. (f) Holloway, R. G.; Penhold, B. R.; Cotton, R.; McCornick, M. J. *J. Chem. Soc., Chem. Commun.* **1976**, 485. (g) Olmstead, M. M.; Benner, L. S.; Hope, H.; Balch, A. L. *Inorg. Chim. Acta* **1979**, *32*, 193. (h) Clark, R. J. H.; Sourisseau, C. *Nouv. J. Chim.* **1980**, *4*, 287. (i) Balch, A. L.; Boehm, J. R.; Hope, H.; Olstead, M. M. *J. Am. Chem. Soc.* **1976**, *98*, 7431. (j) Goldberg, S. Z.; Eisenberg, R. *Inorg. Chem.* **1976**, *15*, 535. (k) Shim, I.; Gingerrich, K. A. *J. Chem. Phys.* **1984**, *80*, 5107, and the references therein.

(38) In the $Ag_2(dmb)_2X_2$ cases (X = Cl, Br, I), the normal mode analysis for cyclic D_{2h} M_2X_2 systems leads to the physically meaningless negative $F(Ag_2)$ values. This is due to the approximations employed for the calculations of very small $F(Ag_2)$ values.